Inorg. Chem. **1993**, *32*, 1749-1755 **1749**

Syntheses and Characterization of Dinuclear Gold(I) Ring and Open-Ring Complexes Containing Saturated and Unsaturated Dithiol Bridging Ligands and Phosphine or Bis(diphosphine) Donor Ligands. Crystal Structures of $[Au_2(\mu\text{-}S(CH_2)_3S)(\mu\text{-dppm})]$, $[Au_2(\mu\text{-MNT})(PPh_3)_2]$, $[Au_2(\mu\text{-}S_2C_6H_4)(PPh_3)_2]$, and $[Au_4(\mu\text{-}S_2C_6H_3CH_3)_2(PEt_3)_2]$

Rosa M. Dávila, Anabel Elduque,[†] Tiffany Grant,[‡] Richard J. Staples, and John P. Fackler, Jr.[*]

Laboratory for Molecular Structure and Bonding, Department of Chemistry, Texas A&M University, College Station, Texas 77843-3255

Received September 10, 1992

Dinuclear gold(I) complexes of the type $[Au_2(\mu\text{-dithiolate})(L)_n]$ where L is a phosphine or bis(dialkylphosphine) have been synthesized. The molecular structures of $[Au_2(\mu\text{-}S(CH_2)_3S)(\mu\text{-dppm})]$ [dppm = bis((diphenylphosphino)-methane)] (**1**), $[Au_2(\mu\text{-MNT})(PPh_3)_2]$ (MNT = 1,2-dicyanoethene-1,2-dithiolate-*S,S′*) (**2**), and $[Au_2(\mu\text{-}S_2C_6H_4)(PPh_3)_2]$ (**3**) are described. In addition, the structure of the tetranuclear bis(dithiolate) $[Au_4(\mu\text{-}S_2C_6H_3CH_3)_2(PEt_3)_2]$ (**4**) is reported. Compound **1** exhibits linear S–Au–P coordination and significant metal–metal interaction, Au···Au = 3.128(1) Å. The open-ring complexes **2** and **3** contain an irregular three-coordinate gold(I) center and a "normal" two-coordinate, linear gold(I) center in contrast to **1**. Compound **4** is a result of $[Au(PEt_3)]^+$ coordination to $[Au_2(\mu\text{-}S_2C_6H_3CH_3)_2]^{2-}$. Pertinent crystal data are as follows: Compound **1** crystallized in the monoclinic space group $C2/c$ with $a = 29.765(9)$ Å, $b = 11.479(2)$ Å, $c = 18.032(4)$ Å, $\beta = 114.65(1)°$, and $V = 5600(2)$ Å^3. Compound **2**·Et_2O crystallized in the space group $P2_1/c$ with $a = 17.663(5)$ Å, $b = 14.185(3)$ Å, $c = 18.780(3)$ Å, $\beta = 114.853(18)°$, and $V = 4269(2)$ Å^3. Compound **3** crystallized in the space group $P2_1$ with $a = 10.761(4)$ Å, $b = 10.687(4)$ Å, $c = 16.227(5)$ Å, $\beta = 98.82(3)°$, and $V = 1844(1)$ Å^3. Compound **4** crystallized in the space group $P2_1$ with $a = 9.767(2)$ Å, $b = 12.373(3)$ Å, $c = 14.096(3)$ Å, $\beta = 92.71(2)°$, and $V = 1707(1)$ Å^3.

Introduction

The synthesis and characterization of dinuclear gold(I) complexes have received much attention in recent years.[1-4] These complexes provide an excellent framework for the study of the weak metal–metal interactions[5,6] observed in gold(I) complexes which are brought about by relativistic effects and how these interactions are affected by the different types of donor ligands used in their synthesis. Homobridged complexes, in particular those containing dithiolate or diphosphine donor ligands, have been the subject of extensive studies.[7-10] The photophysical properties and reactivities that these complexes display which relate to the Au···Au separations have motivated the study of related heterobridged and "open-ring" systems where both dithiolate and bis(dialkylphosphine) or phosphine donor ligands are coordinated to the gold(I) centers.

The study of $[Au_2(\mu\text{-dithiolate})(\mu\text{-diphosphine})]$ and $[Au_2(\mu\text{-dithiolate})(phosphine)_2]$ complexes A and B contributes additionally to our understanding of the chemistry of gold as related to its use in antiarthritic drugs and antitumor agents. The linear S–Au–P coordination generally expected in these compounds is similar to that present in Auranofin and other gold–sulfur drugs which are being used in the treatment of rheumatoid arthritis.[11,12] In addition, the photophysical and photochemical properties of these complexes are of interest due to the large polarizability of the metal–ligand bonds and the observation in many complexes of closed-shell d^{10} ions of visible luminescence arising from a low-lying triplet state. Indeed, it has been suggested that quenching of singlet oxygen by gold(I) compounds may play an important role in the use of gold(I) drugs for rheumatoid arthritis.[13]

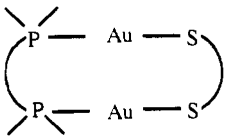

A

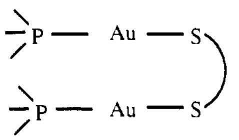

B

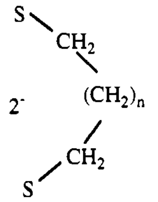

C

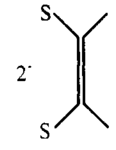

D

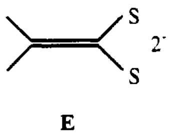

E

---

[*] To whom correspondence should be addressed.

[†] Departamento de Química Inorgaânica, Universidad de Zaragoza, Spain.

[‡] NSF-REU student.

(1) Melník, M.; Parish, R. V. *Coord. Chem. Rev.* **1986**, *70*, 157.

(2) Usón, R.; Laguna, A. *Coord. Chem. Rev.* **1986**, *70*, 1.

(3) Mingos, D. M. P. *Gold Bull.* **1984**, *17*, 5.

(4) Jones, P. G. *Gold Bull.* **1981**, *14*, 102.

(5) Li, J.; Pyykkö, P. *Chem. Phys. Lett.* **1992**, *197*, 586.

(6) Schmidbaur, H. *Gold Bull.* **1990**, *23*, 11.

(7) Jaw, H. R. C.; Meral Savas, M.; Rogers, R. D.; Mason, W. R. *Inorg. Chem.* **1989**, *28*, 1028.

(8) Che, C. M.; Kwong, H. L.; Yam, V. W. W.; Cho, K. C. *J. Chem. Soc., Chem. Commun.* **1989**, 885.

(9) Khan, Md. N. I.; Wang, S.; Fackler, J. P., Jr. *Inorg. Chem.* **1989**, *28*, 3579.

(10) Khan, Md. N. I.; King, C.; Heinrich, D. D.; Fackler, J. P., Jr.; Porter, L. C. *Inorg. Chem.* **1989**, *28*, 2150.

(11) Parish, R. V.; Cottrill, S. M. *Gold Bull.* **1987**, *20*, 3.

(12) Hill, D. T.; Sutton, B. M. *Cryst. Struct. Commun.* **1980**, *9*, 679.

0020-1669/93/1332-1749$04.00/0

We have used dianionic sulfur donor ligands containing both saturated C and unsaturated backbones D. The latter include the 1,2-dithiolenes MNT^{2-}, $[S_2C_6H_4]^{2-}$, and its 3,4-dimercaptotoluene analogue, $[S_2C_6H_3CH_3]^{2-}$. Various 1,2-dithiolenes have been used in the synthesis of mononuclear square planar gold(III) complexes,[14,15] but little work has been directed toward their use as bridging ligands.[16,17] The coordination of $[AuPR_3]^+$ (R = PPh_3) units to the sulfur centers in these ligands has led to very interesting and contrasting structural results which are very different from the results obtained with 1,1-dithiolene ligands, E. Here we report the synthesis and structural characterization of $[Au_2(\mu\text{-}S(CH_2)_3S)(\mu\text{-dppm})]$ (**1**), wherein an intramolecular Au···Au interaction is observed in a 10-membered ring. In the three related 1,2-dithiolene complexes $[Au_2(\mu\text{-MNT})(PPh_3)_2]$ (**2**), $[Au_2(\mu\text{-}S_2C_6H_4)(PPh_3)_2]$ (**3**), and the tetranuclear complex $[Au_4(\mu\text{-}S_2C_6H_3\text{-}CH_3)_2(PEt_3)_2]$ (**4**), an asymmetrical bonding not found in the saturated systems or in the closely related bis(phosphine)(1,1-dithiolato)gold(I) complexes is described.

Experimental Section

All reactions were carried out in oven-dried Schlenk glassware by using standard inert-atmosphere techniques. Infrared spectra (Nujol mulls and KBr pellets) were recorded on a Perkin-Elmer 783 infrared spectrophotometer. NMR spectra were recorded on a Varian XL-200 Fourier transform spectrometer. The $^{31}P\{^1H\}$ NMR are referenced against H_3PO_4. Na_2MNT was prepared according to literature procedures.[18] The compounds[19] $Au(Cl)PPh_3$ and[20] $Au_2(Cl)_2(dppm)$ were prepared by the displacement of THT (THT = tetrahydrothiophene) from Au(Cl)-THT (synthesized according to literature procedure)[21] with PPh_3 and dppm, respectively. 1,3-Propanedithiol, 1,2-benzenedithiol, and 3,4-dimercaptotoluene were commercially available (Aldrich) and used without further purification. Microanalyses were performed by Galbraith Laboratories, Inc.

Preparations. $[Au_2(\mu\text{-}S(CH_2)_3S)(\mu\text{-dppm})]$ (1). To a suspension of $[Au_2(Cl)_2(\mu\text{-dppm})]$ (0.050 g 0.059 mmol) in acetone (10 mL) was added dropwise $KS(CH_2)_3SK$. $KS(CH_2)_3SK$ was prepared in situ by the reaction of $HS(CH_2)_3SH$ (5.9 μL 0.059 mmol) and 2 molar equiv of KOH in MeOH. An immediate reaction was observed with the formation of a colorless solution. After 20 min of stirring, the acetone was concentrated under vacuum. The product was precipitated in MeOH (15 mL). A light yellow solid was obtained. This was filtered off, washed with MeOH and Et_2O, and dried under vacuum; yield 0.052 g (80%). $^{31}P\{^1H\}$ NMR ($CDCl_3$): $\delta = 30.7$ (s). ^1H NMR ($CDCl_3$): $\delta = 2.01$ (m, $SCH_2CH_2CH_2S$), 3.55 (t, $J_{H-H} = 2.2$ Hz, $SCH_2CH_2CH_2S$), 3.65 (t, $J_{P-H} = 16.8$ Hz, CH_2, dppm), 7.55 (m, C_6H_5, dppm). Anal. Calcd for $Au_2S_2P_2C_{28}H_{28}$: C, 38.02; H, 3.19. Found: C, 37.91; H, 3.01.

$[Au_2(\mu\text{-MNT})(PPh_3)_2]$ (2). To a THF solution (5 mL) of Au(Cl)-PPh_3 (0.467 g, 0.944 mmol) was added Na_2MNT (0.0966 g, 0.472 mmol). The solution changed from colorless to yellow. The reaction mixture was stirred for 18 h at room temperature, at which time the THF was evaporated under vacuum, leaving a yellow solid. The solid was dissolved in CH_2Cl_2, and NaCl was filtered off. The CH_2Cl_2 solution was concentrated under vacuum, and a yellow solid was precipitated upon addition of Et_2O (10 mL). The solid was filtered off, washed with Et_2O, and dried under vacuum; yield 0.379 g (76%). IR: 2190 (s, $C{\equiv}N$), 1570 (w), 1580 (w, $C{=}C$, Ph) cm^{-1}. $^{31}P\{^1H\}$ NMR ($CDCl_3$): $\delta = 36.13$ (s). Anal. Calcd for $Au_2S_2P_2N_2C_{40}H_{30}$: C, 45.38; H, 2.86; N, 2.65. Found: C, 42.19; H, 2.84; N, 2.16.

$[Au_2(\mu\text{-}S_2C_6H_4)(PPh_3)_2]$ (3). A MeOH solution containing 1,2-benzenedithiol (0.23 mL, 2.0 mmol) and NaOH (18 mL, 4.7 mmol) was transferred via a cannula into an acetone (10 mL) suspension of $Au(Cl)PPh_3$ (2.00 g, 4.04 mmol). After 4 h, the $Au(Cl)PPh_3$ precipitate was replaced by what appeared as a greenish white precipitate. The solvent was evaporated to dryness, and 10 mL of CH_2Cl_2 was added. The product was partially soluble in CH_2Cl_2. The white solid was filtered off, washed with MeOH and Et_2O, and then vacuum-dried to yield 1.3 g (64%). ^1H NMR ($CDCl_3$): $\delta = 7.65$ (m, C_6H_5), 7.93, 6.86 (AA′BB′, $J_{H-H} = 3.4$ Hz, $J_{H-H} = 5.85$ Hz). $^{31}P\{^1H\}$ NMR ($CDCl_3$) $\delta = 34.70$ (s). Anal. Calcd for $Au_2S_2C_{42}H_{34}$: C, 47.64; H, 3.24. Found: C, 47.23; H, 3.34.

$[Au_4(\mu\text{-}S_2C_6H_3CH_3)_2(PEt_3)_2]$ (4). To a CH_2Cl_2 solution containing $Au(Cl)PEt_3$ (0.1049 g, 0.2992 mmol) was added 3,4-dimercaptotoluene (19.88 μL, 0.1500 mmol). The clear solution was stirred for 16 h at room temperature. At this time, the solvent was concentrated under vacuum and MeOH was added. A white solid precipitated from solution. The solid was filtered off, washed several times with MeOH and Et_2O, and then dried under vacuum; yield 0.0280 g (28%). ^1H NMR ($CDCl_3$): $\delta = 0.91$–0.99 (m, PCH_2CH_3, $J_{H-H} = 7.63$ Hz, $J_{P-H} = 18.25$ Hz), 1.30–1.53 (m, PCH_2CH_3, $J_{P-H} = 16.20$ Hz), 2.28 (s, CH_3), 6.81, 6.84 (d, d; $J_{H-H} = 7.68$ Hz, $J_{H-H} = 1.94$), 7.78 (s, broad), 7.80–7.84 (d). *Note*: Formation of a green solid is observed during the synthesis of **3** and **4**. This is separated from the product through successive washings with MeOH and Et_2O. In the case of **3**, the green product is soluble in CH_2Cl_2 and is also avoided by filtration. Unfortunately, this leads to loss of **3** because it is partially soluble in CH_2Cl_2. It is proposed that this green product is the mononuclear Au(III) oxidized species $[Au(S_2C_6H_4)_2][AuL_2]$ or $[Au(S_2C_6H_3CH_3)_2][AuL_2]$, L = PPh_3 or PEt_3, respectively. The Au(III) product $[Au(S_2C_6H_4)_2][Au(PEt_3)_2]$ has been characterized crystallographically for the reaction of 1,2-benzenedithiol with[22] $Au(Cl)PEt_3$.

X-ray Crystallography. Crystals of **1** suitable for X-ray diffraction analysis were grown by slow diffusion of pentane into a CH_2Cl_2 solution of **1**. Yellow crystals of **2** were grown by slow diffusion of an Et_2O layer into a CH_2Cl_2 solution, and crystals of **3** and **4** were grown by slow evaporation of Et_2O and slow diffusion into a solution of CH_2Cl_2. Crystals were mounted on glass fibers with epoxy cement in a random orientation. Unit cells were determined from 25 machine-centered reflections obtained from rotation photographs and confirmed by axial photographs. Data was collected on a Nicolet R 3m/E diffractometer controlled by a Data General Nova 4 minicomputer using Mo Kα radiation at ambient temperature over the range $4 < 2\theta > 45°$ for the three compounds. The data were corrected for decay, absorption, Lorentz, and polarization effects. All data processing was performed by a Data General Eclipse S140 minicomputer using the SHELXTL crystallographic computational package (version 5.1).

The crystal structure of **1** was solved by using Patterson methods to determine heavy-atom positions, and subsequent atom positions were determined by difference Fourier methods. Convergence to final R values for **1**, $R = 0.0322$ and $R_w = 0.0332$, was obtained by using 4161 reflections $[F^2 \geq 3\sigma(F^2)]$. Compound **1** crystallized in the $C2/c$ space group.

The crystal structures of **2**–**4** were determined by using direct methods. Compound **2** crystallized in the $P2_1/c$ space group, and compound **3**, in $P2_1$, as well as **4**. In each case, the refinements converged uneventfully, giving R values of 0.0432 and 0.0328 for **2** and **3**, respectively. Refinement of the enantiomorph of **3** produced poorer statistics. Structure **4** was solved in $P2_1$; final R values for **4** were $R = 0.0558$ and $R_w = 0.0615$. The enantiomorphic structure refines with poorer statistics. Solution was attempted in space group $P2_1/m$; this offered nonsatisfactory results. This space group implies the presence of an inversion center which is not quite present in the structure.

The fluxional cycles of refinement were performed with hydrogen atoms placed in idealized positions. All non-hydrogen atoms were refined anisotropically (except solvent atoms for compound **2** and carbon atoms for compound **4**). Crystal data and details of the crystallographic experimental parameters are given in Table I. Atomic coordinates and equivalent isotropic thermal parameters for **1**–**4** are presented in Tables II, IV, VI, and VIII, respectively. Relevant bond distances and angles are presented in Tables III, V, VII, and IX, respectively.

Results

The heterobridged complex $[Au_2(\mu\text{-}S(CH_2)_3S)(\mu\text{-dppm})]$ (**1**) was obtained from the reaction of $KS(CH_2)_3SK$ (prepared in situ from the reaction of $HS(CH)_3SH$ with KOH in methanol) and 1 molar equiv of $Au_2(Cl)_2(\mu\text{-dppm})$. The $^{31}P\{^1H\}$ NMR in solution at room temperature shows a singlet at 30.7 ppm, in

---

(13) Corey, E. J.; Mehrotra, M. M.; Khan, A. U. *Science* (*Washington*, D.C.) **1987**, *236*, 68.

(14) Eisenberg, R. *Prog. Inorg. Chem.* **1970**, *12*, 295.

(15) McCleverty, J. A. *Prog. Inorg. Chem.* **1968**, *10*, 49.

(16) Usón, R.; Vicente, J.; Oro, J. *Inorg. Chim. Acta* **1981**, *52*, 29.

(17) Heinrich, D. D.; Fackler, J. P., Jr.; La Huerta, P. *Inorg. Chim. Acta* **1986**, *116*, 15.

(18) Locke, J.; McCleverty, J. A. *Inorg. Chem.* **1966**, *5*, 1157.

(19) McAuliffe, C. A.; Parish, R. V.; Randall, P. D. *J. Chem. Soc., Dalton Trans.* **1979**, 1730.

(20) Schmidbaur, H.; Wohlleben, A.; Wagner, F.; Orama, O.; Huttner, G. *Chem. Ber.* **1977**, *110*, 1748.

(21) Usón, R.; Laguna, A.; Laguna, M. *Inorg. Synth.* **1989**, *26*, 85.

(22) Dávila, R.; Fackler, J. P., Jr. Results to be published.

Table I. Crystallographic Data

formula	$Au_2S_2P_2C_{28}H_{28}$	$Au_2S_2P_2N_2C_{40}H_{30}\cdot C_4H_{10}O$	$Au_2S_2P_2C_{42}H_{34}$	$Au_4S_4P_2C_{26}H_{42}$
fw	884.531	1132.871	1068.974	1332.697
space group	*C*2/*c* (No. 15)	*P*2$_1$/*c* (No. 14)	*P*2$_1$ (No. 4)	*P*2$_1$ (No. 4)
a, Å	29.765(9)	17.664(6)	10.761(4)	9.767(2)
b, Å	11.479(2)	14.186(3)	10.687(4)	12.373(3)
c, Å	18.032(4)	18.780(4)	16.227(5)	14.096(3)
α, deg	90.00	90.00	90.00	90.00
β, deg	114.65(1)	114.85(2)	98.82(3)	92.71(2)
γ, deg	90.00	90.00	90.00	90.00
V, Å^3	5600(2)	4269(2)	1844(1)	1707(1)
Z	8	4	2	2
d_{calc}, g/cm^3	2.10	1.76	1.92	2.59
μ(Mo Kα), cm^{-1}	107.21	70.59	81.6	174.3
λ(radiation),[a] Å	0.710 73	0.710 73	0.710 73	0.710 73
temp, °C	25	25	25	25
transm factor: max, min	0.833, 0.512	0.932, 0.809	0.920, 0.737	0.966, 0.458
R,[b] R_w[c]	0.0322, 0.0332	0.0435, 0.0392	0.0328, 0.0332	0.0558, 0.0615

[a] Graphite-monochromated Mo Kα. [b] $R = \Sigma||F_o| - |F_c||/\Sigma|F_o|$. [c] $R_w = [\Sigma\sqrt{w}(|F_o| - |F_c|)]/\Sigma\sqrt{w}|F_o|$; $w^{-1} = [\sigma^2(|F_o|) + g|F_o|^2]$.

Table II. Atomic Coordinates (×10^4) and Isotropic Thermal Parameters (Å^2 × 10^3)[a] for $[Au_2(\mu\text{-}S_2(CH_2)_3)(\mu\text{-dppm})]$ (**1**)

atom	*x*	*y*	*z*	U_{iso}[b]
Au(1)	4413(1)	251(1)	6662(1)	44(1)
Au(2)	3785(1)	2385(1)	6752(1)	39(1)
S(1)	4990(1)	817(3)	6211(2)	81(2)
S(2)	3907(1)	3310(2)	5727(2)	51(1)
P(1)	3856(1)	−622(2)	7028(1)	35(1)
P(2)	3581(1)	1529(2)	7702(1)	36(1)
C(1)	4676(4)	1729(10)	5310(7)	73(6)
C(2)	4757(4)	3018(10)	5484(8)	74(6)
C(3)	4578(4)	3448(10)	6119(8)	75(6)
C(4)	3788(3)	13(7)	7908(5)	34(3)
C(5)	4029(3)	−2121(7)	7330(5)	34(4)
C(11)	3230(3)	−636(8)	6238(5)	43(4)
C(17)	2916(3)	1490(7)	7388(5)	40(4)
C(23)	3808(3)	2254(7)	8671(6)	41(4)

[a] Estimated standard deviations in the least significant digits are given in parentheses. [b] The equivalent isotropic *U* is defined as one-third of the trace of the $\mathbf{U}_{ij}$ tensor.

Table III. Bond Lengths (Å) and Angles (deg)[a] for $[Au_2(\mu\text{-}S_2(CH_2)_3)(\mu\text{-dppm})]$ (**1**)

Au(1)–Au(2)	3.128(1)	Au(1)–S(1)	2.281(4)
Au(1)–P(1)	2.259(3)	Au(2)–S(2)	2.288(3)
Au(2)–P(2)	2.266(3)	S(1)–C(1)	1.828(11)
S(2)–C(3)	1.827(11)	P(1)–C(4)	1.833(10)
P(1)–C(5)	1.814(8)	P(1)–C(11)	1.812(8)
P(2)–C(4)	1.832(8)	P(2)–C(17)	1.818(10)
P(2)–C(23)	1.793(9)	C(1)–C(2)	1.512(16)
C(2)–C(3)	1.532(22)		
Au(2)–Au(1)–S(1)	110.5(1)	Au(2)–Au(1)–P(1)	78.7(1)
S(1)–Au(1)–P(1)	170.0(1)	Au(1)–Au(2)–S(2)	91.3(1)
Au(1)–Au(2)–P(2)	93.1(1)	S(2)–Au(2)–P(2)	174.1(1)
Au(1)–S(1)–C(1)	107.3(5)	Au(2)–S(2)–C(3)	104.1(4)
Au(1)–P(1)–C(4)	115.9(3)	Au(1)–P(1)–C(5)	110.9(3)
C(4)–P(1)–C(5)	103.7(4)	Au(1)–P(1)–C(11)	114.4(4)
C(4)–P(1)–C(11)	103.6(4)	C(5)–P(1)–C(11)	107.3(4)
Au(2)–P(2)–C(4)	113.1(4)	Au(2)–P(2)–C(17)	112.0(3)
C(4)–P(2)–C(17)	105.6(4)	Au(2)–P(2)–C(23)	115.1(3)
C(4)–P(2)–C(23)	106.6(4)	C(17)–P(2)–C(23)	103.5(5)
S(1)–C(1)–C(2)	113.4(8)	C(1)–C(2)–C(3)	113.3(12)
S(2)–C(3)–C(2)	110.4(7)	P(1)–C(4)–P(2)	110.6(5)

[a] Estimated standard deviations in the least significant digits are given in parentheses.

Table IV. Atomic Coordinates (×10^4) and Isotropic Thermal Parameters (Å^2 × 10^3)[a] for $[Au_2(S_2C_2(CN)_2)(PPh_3)_2]\cdot Et_2O$ (**2**)

atom	*x*	*y*	*z*	U_{iso}[b]
Au(1)	1949(1)	5643(1)	−667(1)	42(1)
Au(2)	3153(1)	5479(1)	−1488(1)	37(1)
S(1)	1355(3)	7020(3)	−1341(3)	60(2)
S(2)	3474(2)	6494(3)	−431(2)	40(2)
P(1)	2063(3)	4273(3)	−2(2)	38(2)
P(2)	2899(3)	4382(3)	−2440(2)	37(2)
N(1)	1727(11)	9444(10)	−1735(11)	94(11)
N(2)	4069(10)	8875(12)	−757(10)	80(10)
C(1)	2174(11)	7769(11)	−1216(9)	39(8)
C(2)	3011(11)	7562(10)	−864(9)	40(9)
C(3)	1902(11)	8714(13)	−1520(10)	50(9)
C(4)	3603(12)	8316(11)	−803(10)	47(9)
C(5)	3120(9)	4036(10)	654(10)	42(8)
C(11)	1462(8)	4341(11)	593(8)	36(7)
C(17)	1705(10)	3208(11)	−560(9)	39(9)
C(23)	1812(9)	4304(11)	−3077(9)	40(7)
C(29)	3412(9)	4528(12)	−3085(9)	42(8)
C(35)	3211(10)	3239(10)	−1995(8)	39(8)

[a] Estimated standard deviations in the least significant digits are given in parentheses. [b] The equivalent isotropic *U* is defined as one-third of the trace of the $\mathbf{U}_{ij}$ tensor.

Table V. Bond Lengths (Å) and Angles (deg)[a] for $[Au_2(S_2C_2(CN)_2)(PPh_3)_2]\cdot Et_2O$ (**2**)

Au(1)–Au(2)	3.115(3)	Au(1)–S(1)	2.323(4)
Au(1)–S(2)	2.811(5)	Au(1)–P(1)	2.273(4)
Au(2)–S(2)	2.321(4)	Au(2)–S(1)	3.958(5)
Au(2)–P(2)	2.269(4)	S(1)–S(2)	3.479(6)
S(1)–C(1)	1.729(18)	S(2)–C(2)	1.751(15)
P(1)–C(5)	1.784(14)	P(1)–C(11)	1.839(19)
P(1)–C(17)	1.795(16)	P(2)–C(23)	1.788(13)
P(2)–C(29)	1.803(20)	P(2)–C(35)	1.800(15)
N(1)–C(3)	1.108(23)	N(2)–C(4)	1.119(26)
C(1)–C(2)	1.372(24)	C(1)–C(3)	1.456(23)
C(2)–C(4)	1.466(26)		
S(1)–Au(1)–P(1)	158.9(2)	S(2)–Au(2)–P(2)	174.7(1)
Au(1)–S(1)–C(1)	106.4(5)	Au(2)–S(2)–C(2)	103.9(5)
Au(1)–P(1)–C(5)	111.4(6)	Au(1)–P(1)–C(11)	110.4(5)
C(5)–P(1)–C(11)	107.1(8)	Au(1)–P(1)–C(17)	118.0(6)
C(5)–P(1)–C(17)	104.8(7)	C(11)–P(1)–C(17)	104.4(8)
Au(2)–P(2)–C(23)	111.8(6)	Au(2)–P(2)–C(29)	117.5(5)
C(23)–P(2)–C(29)	105.0(7)	Au(2)–P(2)–C(35)	109.3(5)
C(23)–P(2)–C(35)	106.8(7)	C(29)–P(2)–C(35)	105.9(8)
S(1)–C(1)–C(2)	127.1(12)	S(1)–C(1)–C(3)	113.1(12)
C(2)–C(1)–C(3)	119.8(15)	S(2)–C(2)–C(1)	127.4(14)
S(2)–C(2)–C(4)	114.6(12)	C(1)–C(2)–C(4)	118.0(13)
N(1)–C(3)–C(1)	177.2(20)	N(2)–C(4)–C(2)	178.3(21)

[a] Estimated standard deviations in the least significant digits are given in parentheses.

agreement with a symmetrical arrangement of linear S–Au–P units, consistent with the structure of the solid.

The reaction between $Au(Cl)PPh_3$ and Na_2MNT in THF produced $[Au_2(MNT)(PPh_3)_2]$ (**2**) in 76% yield. The IR spectrum shows the CN stretching frequency at 2190 cm^{-1}, indicating the presence of the MNT ligand. The complex is stable at room temperature. An analogous type of complex, $[Au_2(\mu\text{-}S_2C_6H_4)(PPh_3)_2]$ (**3**), was synthesized by the reaction of 1,2-benzenedithiol (deprotonated by using a methanolic solution of KOH) and 2 molar equiv of $Au(Cl)PPh_3$. This complex is also stable at room temperature. The ^{1}H NMR of this complex shows a multiplet at 7.65 ppm corresponding to the phenyl rings of the

Table VI. Atomic Coordinates (×10⁴) and Isotropic Thermal Parameters (Å² × 10³)[a] for $[Au_2(\mu\text{-}S_2C_6H_4)(PPh_3)_2]$ (**3**)

atom	*x*	*y*	*z*	U_{iso}[b]
Au(1)	6931(1)	4539	7950(1)	34(1)
Au(2)	4622(1)	3758(1)	6615(1)	32(1)
S(1)	7824(4)	2556(4)	8059(3)	50(1)
S(2)	6614(3)	4081(4)	6277(2)	35(1)
P(1)	6358(3)	6453(4)	8333(2)	31(1)
P(2)	2640(3)	3350(3)	6846(2)	32(1)
C(1)	7729(12)	1947(13)	7065(8)	34(5)
C(2)	7173(14)	2506(14)	6321(9)	39(5)
C(3)	7129(18)	1889(18)	5552(11)	64(7)
C(4)	7580(21)	738(18)	5489(12)	77(8)
C(5)	8150(16)	149(16)	6225(12)	69(8)
C(6)	8208(14)	701(18)	6996(9)	53(6)
C(10)	7644(13)	7335(15)	8939(8)	35(5)
C(20)	5742(12)	7452(14)	7466(7)	33(5)
C(30)	5134(12)	6442(15)	8996(7)	33(5)
C(40)	2545(12)	2030(13)	7542(8)	29(4)
C(50)	1876(12)	4656(15)	7253(8)	36(4)
C(60)	1668(11)	2900(15)	5907(9)	36(5)

[a] Estimated standard deviations in the least significant digits are given in parentheses. [b] The equivalent isotropic *U* is defined as one-third of the trace of the U_{ij} tensor.

Table VII. Bond Lengths (Å) and Angles (deg)[a] for $[Au_2(\mu\text{-}S_2C_6H_4)(PPh_3)_2]$ (**3**)

Au(1)–Au(2)	3.148(2)	Au(1)–S(1)	2.322(4)
Au(1)–S(2)	2.727(3)	Au(1)–P(1)	2.252(4)
Au(2)–S(1)	4.067(4)	Au(2)–S(2)	2.319(4)
Au(2)–P(2)	2.263(4)	S(1)–S(2)	3.400(6)
S(1)–C(1)	1.728(14)	S(2)–C(2)	1.785(15)
P(1)–C(10)	1.831(14)	P(1)–C(20)	1.808(13)
P(1)–C(30)	1.823(14)	P(2)–C(40)	1.820(14)
P(2)–C(50)	1.796(15)	P(2)–C(60)	1.778(13)
C(1)–C(2)	1.396(19)	C(1)–C(6)	1.438(24)
C(2)–C(3)	1.406(24)	C(3)–C(4)	1.331(28)
C(4)–C(5)	1.405(26)	C(5)–C(6)	1.375(25)
S(1)–Au(1)–S(2)	84.2(1)	S(1)–Au(1)–P(1)	159.3(1)
S(2)–Au(1)–P(1)	116.1(1)	S(2)–Au(2)–P(2)	175.3(1)
Au(1)–S(1)–C(1)	107.9(5)	Au(1)–S(2)–Au(2)	76.8(1)
Au(1)–S(2)–C(2)	98.0(5)	Au(2)–S(2)–C(2)	99.7(5)
Au(1)–P(1)–C(10)	113.5(5)	Au(1)–P(1)–C(20)	113.8(5)
C(10)–P(1)–C(20)	105.7(7)	Au(1)–P(1)–C(30)	114.2(5)
C(10)–P(1)–C(30)	104.0(6)	C(20)–P(1)–C(30)	104.5(6)
Au(2)–P(2)–C(40)	113.3(4)	Au(2)–P(2)–C(50)	114.1(5)
C(40)–P(2)–C(50)	107.6(7)	Au(2)–P(2)–C(60)	110.8(5)
C(40)–P(2)–C(60)	103.9(6)	C(50)–P(2)–C(60)	106.4(6)
S(1)–C(1)–C(2)	127.0(11)	S(1)–C(1)–C(6)	116.8(10)
C(2)–C(1)–C(6)	116.1(12)	S(2)–C(2)–C(1)	122.3(11)
S(2)–C(2)–C(3)	116.2(12)		

[a] Estimated standard deviations in the least significant digits are given in parentheses.

Table VIII. Atomic Coordinates (×10⁴) and Equivalent Isotropic Displacement Parameters (Å² × 10³)[a] for $[Au_4(\mu\text{-}S_2C_6H_3CH_3)_2(PEt_3)_2]$ (**4**)

atom	*x*	*y*	*x*	*U*(eq)[b]
Au(1)	9668(2)	12340(8)	1551(1)	72(1)
Au(2)	5462(2)	11315(8)	3528(1)	67(1)
Au(3)	6776(2)	11329(8)	1635(1)	64(1)
Au(4)	8366(2)	12336(8)	3481(1)	67(1)
S(1)	8982(12)	13791(9)	2572(8)	81(2)
S(2)	7239(12)	12726(12)	616(9)	89(2)
S(2)	6186(10)	9816	2547(8)	83(2)
S(4)	7858(11)	10945(13)	4492(9)	87(2)
P(1)	11054(11)	10982(12)	1097(8)	74(2)
P(2)	4112(11)	12619(13)	4011(9)	87(2)
C(1)	7266(28)	14383(28)	2003(25)	112(3)
C(2)	6663(27)	13991(26)	1230(23)	83(3)
C(3)	5550(27)	14466(27)	802(24)	108(3)
C(4)	4921(28)	15406(28)	1046(23)	103(3)
C(5)	5580(26)	15759(26)	1819(22)	80(3)
C(6)	6593(29)	15355(29)	2436(25)	129(3)
C(7)	5121(28)	17007(27)	2057(24)	129(3)
C(8)	7720(23)	9434(23)	3120(19)	53(3)
C(9)	8335(26)	9848(25)	3940(21)	73(3)
C(10)	9763(29)	9314(28)	4387(24)	122(3)
C(11)	9925(29)	8342(28)	3786(24)	119(3)
C(12)	9581(27)	7984(27)	3091(23)	97(3)
C(13)	8155(26)	8472(25)	2645(21)	80(3)
C(14)	10288(28)	6977(27)	2656(23)	122(3)
C(15)	11681(26)	10211(25)	1976(21)	79(3)
C(17)	10468(29)	10068(29)	295(25)	160(3)
C(19)	12348(31)	11358(31)	465(30)	268(3)
C(21)	2295(28)	12198(28)	4243(25)	131(3)
C(23)	5302(27)	13832(26)	4677(21)	86(3)
C(25)	3426(28)	13643(28)	2777(22)	110(3)

[a] Estimated standard deviations are given in parentheses. [b] Equivalent isotropic *U* defined as one-third of the trace of the orthogonalized U_{ij} tensor.

PPh_3. An AA′BB′ system is observed at 7.93 and 6.86 ppm for the hydrogens of the bridging dithiolene. The J_{H-H} values are 3.40 and 5.86 Hz, respectively. For compound **4**, the ^1H NMR agrees with coordination of $[AuPEt_3]^+$ to the 1,2-dithiolene. The coordination of the 3,4-dimercaptotoluene ligand is confirmed, and an upfield shift of the PEt_3 signals with respect to Au(Cl) PEt_3 [$\delta(PCH_2CH_3)$ = 1.06–1.23 (m) and $\delta(PCH_2CH_3)$ = 1.73–1.89 (m)] is observed.

Crystal Structure Descriptions

$[Au_2(\mu\text{-}S(CH_2)_3S)(\mu\text{-dppm})]$ (1). The molecular structure of **1** is shown in Figure 1. The two gold atoms are bridged on one side by one bis(diphenylphosphino)methane ligand, Au(1)–P(1) = 2.259(3) Å and Au(2)–P(2) = 2.266(3) Å, and on the other side by one 1,3-propanedithiolate ligand, Au(1)–S(1) = 2.281(4) Å and Au(2)–S(2) = 2.288(3) Å. The Au–P and Au–S bond lengths are typical for these type of complexes. The coordination of the gold atoms to the bridging ligands is almost linear: S(1)–Au(1)–P(1) = 170.0(1)°; S(2)–Au(2)–P(2) = 174.1(1)°. The Au(1)–Au(2) distance of 3.128(1) Å indicates metal–metal interaction.

$[Au_2(\mu\text{-MNT})(PPh_3)_2]$ (2). The molecular structure of **2** is shown in Figure 2. The two gold atoms are bridged by an MNT ligand bonded through the sulfur atoms, Au(1)–S(1) = 2.323(4) Å and Au(2)–S(2) = 2.321(4) Å. Each gold(I) center is coordinated to a PPh_3 unit, Au(1)–P(1) = 2.273(4) Å and Au(2)–P(2) = 2.269(4) Å.

The coordination around Au(2) is linear, S(2)–Au(2)–P(2) = 174.7(1)°, as expected for this type of complex. On the other hand, the coordination around Au(1) deviates considerably from linearity, S(1)–Au(1)–P(1) = 158.9(2)°. Figure 3 presents a clearer view of the metal centers. A bonding interaction between S(2) and Au(1) of 2.811(3) Å is observed.

$[Au_2(\mu\text{-}S_2C_6H_4)(PPh_3)_2]$ (3). A structure analogous to that obtained for compound **2** was observed for complex **3**. The molecular structure is shown in Figure 4. Again, the two gold atoms are bridged by the 1,2-dithiolene ($\mu\text{-}S_2C_6H_4$) and each one is coordinated to a PPh_3 unit with typical Au–S and Au–P distances: Au(1)–P(1) = 2.252(4) Å, Au(1)–S(1) = 2.322(4) Å, Au(2)–P(2) = 2.263(4) Å, Au(2)–S(2) = 2.319(4) Å. Au(2) exhibits a linear coordination, S(2)–Au(2)–P(2) = 175.3(1)°, while the coordination around Au(1) deviates from linearity, S(1)–Au(1)–P(1) = 159.3(1)°. A bonding interaction between S(2) and the opposite gold [Au(1)] center is observed.

$[Au_2(S_2C_6H_3CH_3)_2(PEt_3)_2]$ (4). Figure 5 shows the molecular structure for complex **4**. This molecule is a rectangular array of four gold atoms which are in the same plane (slight deviation of 0.0052 Å) and which are within interacting distances from one another ranging from 3.02 to 3.23 Å: Au(1)–Au(3) = 3.104(6) Å, Au(1)–Au(4) = 3.058(3) Å, Au(2)–Au(3) = 3.017(3) Å, Au(2)–Au(4) = 3.116(6) Å, Au(3)–Au(4) = 3.219(6) Å. The two dithiolene units are bridging the central gold atoms: Au(4)–S(4) = 2.30(2) Å, Au(3)–S(3) = 2.36(1) Å, Au(4)–S(1) =

Table IX. Bond Lengths (Å) and Angles (deg)[a] for $[Au_4(\mu\text{-}S_2C_6H_3CH_3)_2(PEt_3)_2]$ (**4**)

Au(1)–Au(3)	3.104(6)	Au(1)–Au(4)	3.058(3)
Au(1)–S(1)	2.42(1)	Au(1)–S(2)	2.71(1)
Au(1)–P(1)	2.27(1)	Au(2)–Au(3)	3.017(3)
Au(2)–Au(4)	3.116(6)	Au(2)–S(3)	2.44(1)
Au(2)–S(4)	2.69(1)	Au(2)–P(2)	2.21(2)
Au(3)–Au(4)	3.219(6)	Au(3)–S(2)	2.31(2)
Au(3)–S(3)	2.36(1)	Au(4)–S(1)	2.31(1)
Au(4)–S(4)	2.30(2)	S(1)–C(1)	1.97(3)
S(2)–C(2)	1.89(3)	S(3)–C(8)	1.74(2)
S(4)–C(9)	1.64(3)	P(1)–C(15)	1.66(3)
P(1)–C(17)	1.68(4)	P(1)–C(19)	1.65(4)
P(2)–C(21)	1.90(3)	P(2)–C(23)	2.10(3)
P(2)–C(25)	2.23(3)	C(1)–C(2)	1.31(4)
C(8)–C(9)	1.38(4)		

S(1)–Au(1)–S(2)	84.1(4)	S(1)–Au(1)–P(1)	154.8(4)
S(2)–Au(1)–P(1)	121.1(5)	S(3)–Au(2)–S(4)	83.5(4)
S(3)–Au(2)–P(2)	157.3(4)	S(4)–Au(2)–P(2)	119.2(5)
S(2)–Au(3)–S(3)	174.2(5)	S(1)–Au(4)–S(4)	175.2(5)
Au(1)–S(1)–Au(4)	80.7(4)	Au(1)–S(1)–C(1)	107(1)
Au(4)–S(1)–C(1)	106(1)	Au(1)–S(2)–Au(3)	76.0(4)
Au(1)–S(2)–C(2)	101(1)	Au(3)–S(2)–C(2)	105(1)
Au(2)–S(3)–Au(3)	77.9(2)	Au(2)–S(3)–C(8)	102(1)
Au(3)–S(3)–C(8)	104(1)	Au(2)–S(4)–Au(4)	76.7(4)
Au(2)–S(4)–C(9)	99(1)	Au(4)–S(4)–C(9)	104(1)
Au(1)–P(1)–C(15)	115(1)	Au(1)–P(1)–C(17)	120(1)
C(15)–P(1)–C(17)	103(2)	Au(1)–P(1)–C(19)	115(1)
C(15)–P(1)–C(19)	107(2)	C(17)–P(1)–C(19)	94(2)
Au(2)–P(2)–C(21)	116(1)	Au(2)–P(2)–C(23)	109.4(9)
C(21)–P(2)–C(23)	129(1)	Au(2)–P(2)–C(25)	110(1)
C(21)–P(2)–C(25)	92(1)	C(23)–P(2)–C(25)	95(1)
S(1)–C(1)–C(2)	123(2)	S(1)–C(1)–C(6)	121(2)
S(2)–C(2)–C(1)	124(2)	S(2)–C(2)–C(3)	114(2)
S(3)–C(8)–C(9)	129(2)	S(3)–C(8)–C(13)	106(2)
S(4)–C(9)–C(8)	126(2)	S(4)–C(9)–C(10)	114(2)

[a] Estimated standard deviations are given in parentheses.

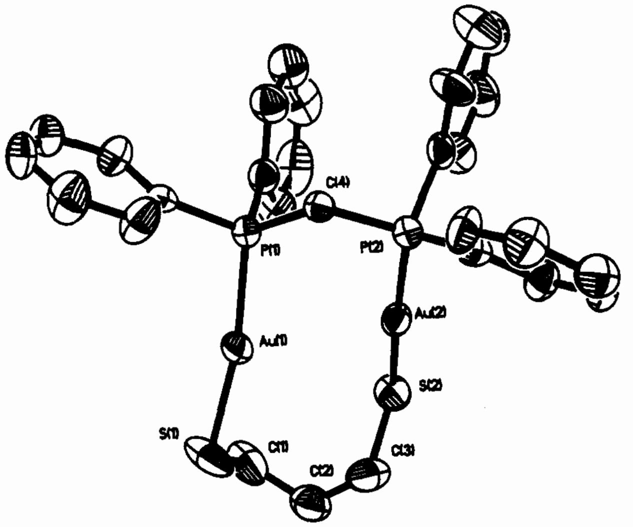

Figure 1. Perspective view of $[Au_2(\mu\text{-}S(CH_2)_3S)(dppm)]$ (**1**) showing the atomic labeling scheme at 50% probability.

2.31(1) Å, Au(3)–S(2) = 2.31(2) Å. The $AuPEt_3$ units appear to be capping the central Au–S plane. Au(2)–P(2) = 2.21(2) Å, Au(1)–P(1) = 2.27(1) Å, S(3)–Au(2)–S(4) = 83.5(4)°, S(2)–Au(1)–S(1) = 84.1(4)°.

Discussion

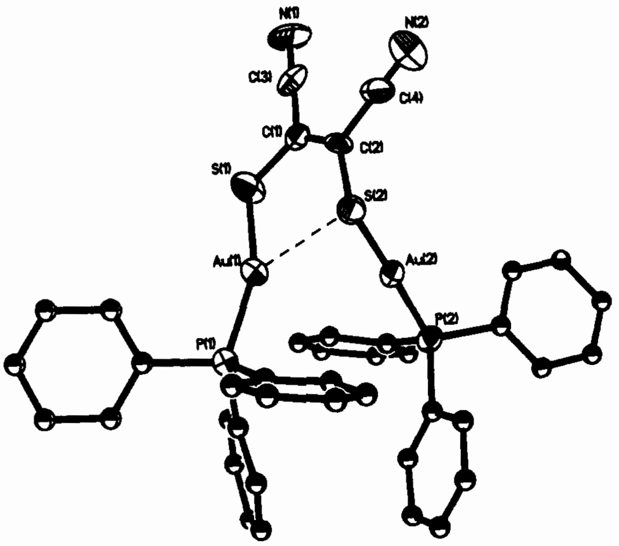

Figure 2. Perspective view of $[Au_2(\mu\text{-MNT})(PPh_3)_2]$ (**2**) showing the atomic labeling scheme at 30% probability. Phenyl rings have been fixed to arbitrary radii for clarity.

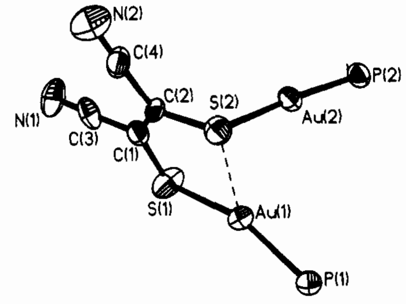

Figure 3. Partial view of $[Au_2(\mu\text{-MNT})(PPh_3)_2]$ (**2**) (phenyl rings omitted for clarity) showing the Au(1)–S(2) interaction [Au(1)–S(2) = 2.810 Å]. Au(1) is an irregular three-coordinate gold(I) center while Au(2) is a normal two-coordinate linear gold center.

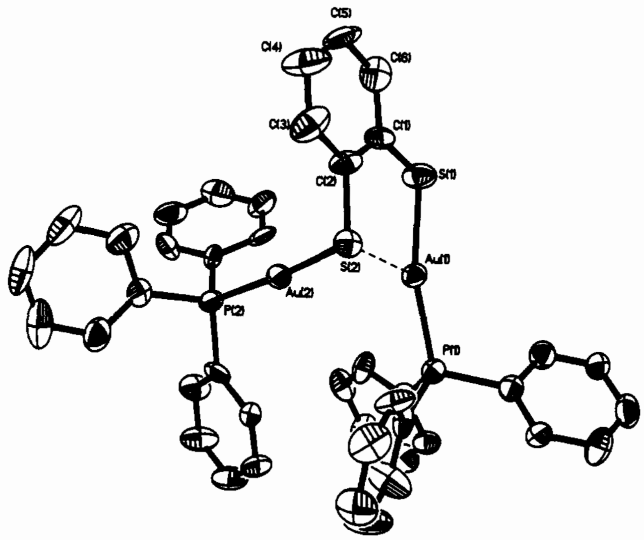

Figure 4. Perspective view of $[Au_2(\mu\text{-}S_2C_6H_4)(PPh_3)_2]$ (**3**) showing the atomic labeling scheme at 50% probability.

It is well-known that gold(I) tends to form linear two-coordinate complexes.[23] There are also numerous examples of dinuclear gold(I) ring complexes reported in the literature where the linear coordination around gold(I) centers is maintained.[4,9,24] In many cases the rings are eight-membered, consisting of the two metal atoms, four donor atoms, and a bridging atom connecting pairs of these coordinating atoms. Compound **1** shows that an expansion of the eight-membered ring system to a ten-membered ring still gives a close Au···Au contact of 3.128(1) Å. While nearly linear S–Au–P units are observed, there is a slight deviation from

---

(23) Puddephatt, H. R. In *Comprehensive Coordination Chemistry*; Wilkinson, G., Gillard, R. D., McCleverty, J. A., Eds.; Pergamon Press: Oxford, England, 1987; Vol. 5, p 861.

(24) Hall, K. P.; Mingos, D. M. P. *Prog. Inorg. Chem.* **1984**, *32*, 237.

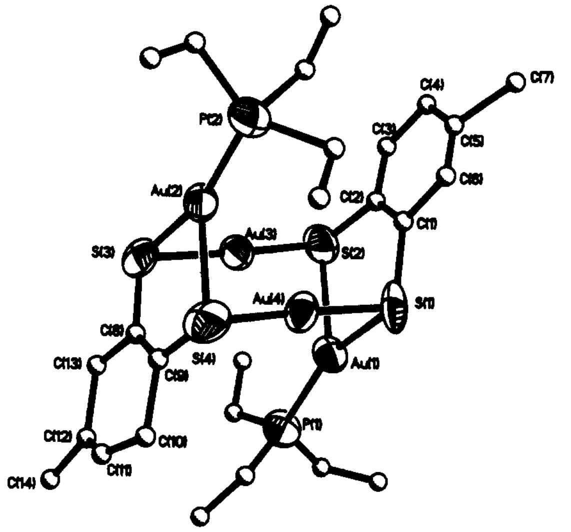

Figure 5. Perspective view of $[Au_2(S_2C_6H_3CH_3)_2(PEt_3)_2]$ (**4**) showing the atomic labeling scheme at 50% probability. The 3,4-dimercaptotolune ligands and the ethyl groups have been fixed to arbitrary radii for clarity.

linearity, 6–10°, probably due to the twist of the propylene chain, which is needed to maintain the Au···Au contacts. On the basis of elegant arguments related to the relative energies of different structural configurations of dinuclear gold(I) compounds, Schmidbaur[3,25] has estimated the Au···Au interaction to be 6–8 kcal/mol, about as strong as hydrogen bonds in water. Preliminary photophysical studies of compound **1** indicate that in the solid state this complex is luminescent under ultraviolet radiation at room temperature. Luminescence is frequently found in dinuclear gold(I) systems.[26] Studies of the photophysics of these complexes are currently under progress, and the results will be reported elsewhere.

Little work has been reported to date dealing with bridging dithiolene ligands. A few years ago[9,10] we reported studies with the 1,1-dithiolene ligand *i*-MNT, $[S_2CC(CN)_2]^{2-}$. We found that the eight-membered ring complex $[Au_2(i\text{-MNT})_2]^{2-}$ oxidized to form a metal–metal-bonded gold(II) species. We were interested to know if 1,2-dithiolene ligands such as MNT^{2-}, $[S_2C_6H_4]^{2-}$, and $[S_2C_6H_3CH_3]^{2-}$ would show a similar formation of a metal–metal bond. These ligands had been studied extensively in the synthesis and electron-transfer reactions of mononuclear square planar complexes.[14,27,28]

The structural characterization of $[Au_2(i\text{-MNT})(PPh_3)_2]$ showed[29] this complex to exhibit a symmetrical arrangement wherein both S–Au–P angles are approximately linear, 172(1)°. Thus we expected this type of geometry to be present in compounds **2** and **3**, as also found in **1**, but this is not the case. The structures of **2** and **3** are very unsymmetrical and somewhat reminiscent (diagram I) of the structure reported[17] several years ago for the silver(I) complex of MNT, $Ag_2(\mu\text{-MNT})(PPh_3)_4$. However, this latter complex has a four-coordinate Ag(I) atom bonded nearly symmetrically to the two S atoms of the MNT and two P atoms with a three-coordinate Ag(I) atom bonded to one of the dithiolate S atoms and two P atoms (I). Furthermore, the Ag···Ag separation is 4.392 Å. The interaction between S(2) of the bridging dithiolene in **2** and **3** and the opposite gold(I) center [Au(1)] approaches the interaction observed in the silver compound. The values of the bond distances and angles around Au(1) imply an irregular three-coordinate gold(I) atom,[4] while the other gold(I) atom is essentially two-coordinate (excluding the close Au···Au contact 3.115(3) Å.

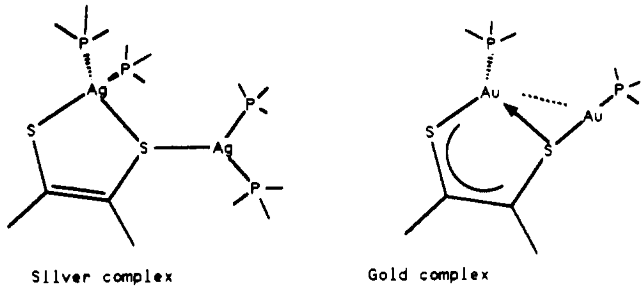

I

Other examples of three-coordinate gold(I) complexes have been reported in the literature.[30–32] The special features of complexes **2**–**4** reside in the differences they show from 1,1-dithiolenes and the heterobridged complexes containing saturated dithiolates. Presumably because of the changes in the electron density at the sulfur atoms, the gold(I) complexes of the saturated dithiolates and the 1,1-dithiolates do not exhibit interactions between gold and a second sulfur atom of the bridging ligand as observed with 1,2-dithiolene ligands. Although steric factors due to the presence of the bulky PPh_3 ligands also may be involved to help account for the differences observed in structural features, the electronic factors appear to be more important. Indeed, preliminary structural results indicate that the structures of the triethylphosphine and trimethylphosphine derivatives are quite similar, ruling out steric arguments as the cause for the observed structural differences.

Table X shows selected bond distances of the 1,1-dithiolene and 1,2-dithiolene complexes and the heterobridged complex **1**. The metal–metal distances for complexes **2** and **3** are smaller than the sum of the van der Waals radii for gold [Au(1)–Au(2) = 3.116(3) Å, **1**; Au(1)–Au(2) = 3.1489(6) Å, **2**] and substantially smaller than the Ag···Ag separation, illustrating the relativistic gold–gold bond common for dinuclear gold(I) complexes.[3] It is interesting to note that the M–M distance does not vary significantly in these gold(I) complexes while the bite distance (S–S) of the sulfur ligand changes considerably, increasing from the 1,1-dithiolene to the 1,2-dithiolenes and the saturated dithiolate. The observed Au···Au separation in various dithio complexes range from about 2.76 Å in the dithiocarbamates[33,34] to the 3.3-Å separation found in **4**.

It is well-known that dithiolene complexes are capable of undergoing facile electron-transfer reactions. It is possible that coordination of $[AuPPh_3]^+$ to the 1,2-dithiolenes allows for partial oxidation of the ligand. (The electronegativity of the gold atom, 2.54 on the Pauling scale, is large compared with that of silver, 1.93.) This in effect removes some electron density from the highest filled π orbital of the ligand, a mainly antibonding orbital which is π bonding in the C–C bond. Scheme I attempts to describe this effect. The residual electron density on the sulfur [S(2)] is donated from the sulfur to the opposite gold center [Au(1)]. This gold center in turn contributes electron density back into the adjacent sulfur [S(1)], causing electron delocalization across the ligand backbone, giving a type of unsymmetrical

---

(25) Schmidbaur, H. In *Unkonventionelle Wechselwirkungen in der Chemie metallischer Elemente*; Krebs, B., Ed.; VCH Verlagsgesellschaft: Weinheim, Germany, 1992; Part C3, p 378.

(26) King, C.; Wang, J. C.; Khan, Md. N. I.; Fackler, J. P., Jr. *Inorg. Chem.* **1989**, *28*, 2145.

(27) Davison, A.; Edelstein, N.; Holm, R. H.; Maki, A. H. *Inorg. Chem.* **1963**, *2*, 1227.

(28) Baker-Hawkes, M. J.; Billig, E.; Gray, H. B. *J. Am. Chem. Soc.* **1966**, *88*, 4870.

(29) Khan, Md. N. I.; Wang, S.; Heinrich, D. D.; Fackler, J. P., Jr. *Acta Crystallogr., Sect. C* **1988**, *C44*, 822.

(30) Wijnhoven, J. G.; Bosman, W. P. J. H.; Beursken, P. T. *J. Cryst. Mol. Struct.* **1972**, *2*, 7.

(31) Jones, P. G.; Sheldrick, G. M.; Fügner, A.; Götzfried, F.; Beck, W. *Chem. Ber.* **1981**, *114*, 1413.

(32) Bensch, W.; Prelati, M.; Ludwig, W. *J. Chem. Soc., Chem. Commun.* **1986**, 1762.

(33) Hesse, R.; Jennische, P. *Acta Chem. Scand.* **1972**, 3855.

(34) Jennische, P.; Anacker-Eickhoff, H.; Wahlberg, A. *Acta Crystallogr., Sect. A* **1975**, *A31*, S143.

Scheme I

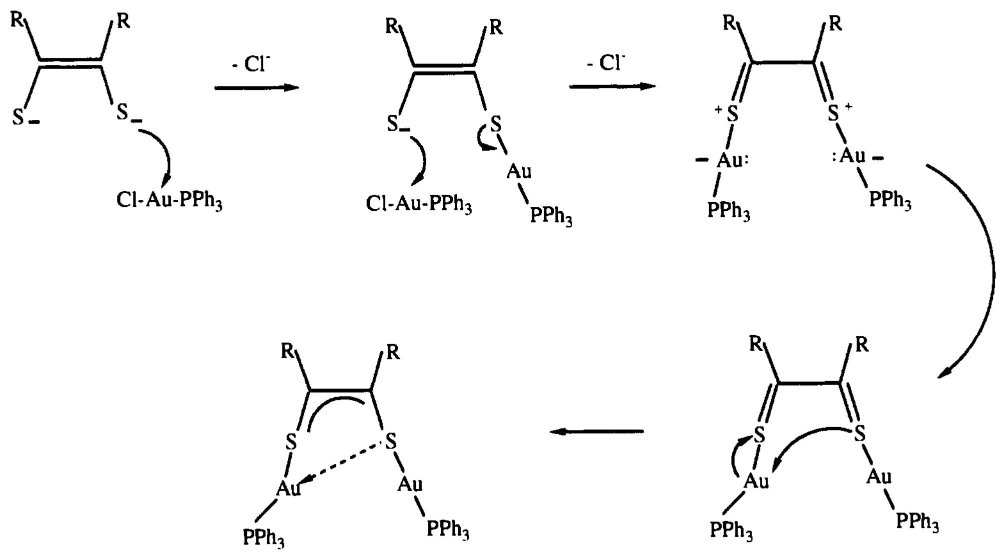

Table X. Comparison of Bond Distances (Å) for Open-Ring and Heterobridged Complexes

complex	Au···Au	S···S	Au–S	C–S
$[Au_2(\mu\text{-}S(CH)_3S)(dppm)]$ (**1**)	3.128(1)	4.122(4)	2.281(4)	1.828(11)
			2.288(3)	1.827(11)
$[Au_2(i\text{-}MNT)(PPh_3)_2]$[25]	3.156(1)	3.043(6)	2.313(2)	1.729(7)
$[Au_2(MNT)(PPh_3)_2]$ (**2**)	3.116(3)	3.490(5)	2.323(4)	1.729(18)
			2.321(4)	1.751(15)
$[Au_2(\mu\text{-}S_2C_6H_4)(PPh_3)_2]$ (**3**)	3.1489(6)	3.399(5)	2.319(4)	1.728(14)
				1.785(15)

allylic thiol electronic arrangement. The latter electronic organization would explain the shortening of one of the C–S bond distances and the elongation of the other in all three 1,2-dithiolene complexes, reminiscent of the observations made in the structures of organic thiones when coordinated to gold(I).[35] The formation of two dipoles upon partial oxidation of the ligand allows one of the sulfur atoms [S(2)] to be pushed out from the plane of the other sulfur and gold atoms and facilitates an interaction with one of the empty p orbitals of the opposite gold(I) center. The coordination sphere around one of the Au(I) centers apparently is not satisfied by two-coordination. This further supports the idea that electron delocalization and partial charge separation are important in these ligand systems, which are different from the situation with saturated dithiols or the unsaturated 1,1-dithiols.

With the 3,4-dimercaptotoluene ligand, dimerization is observed to produce a species more like $[Au_2(i\text{-}MNT)_2]^{2-}$ but with $[Au(PEt_3)]^+$ coordinated to two of the four sulfur atoms. The extra electron-donating capacity of this ligand compared with $[MNT]^{2-}$ allows more electron density to be pushed onto the metal atoms. Relativistic gold–gold bonds occur between the gold(I) atoms, giving rise to a four-atom gold chain. The ten-membered ring takes on the form of a chair. Oxidative addition with halogens, as observed with $[Au_2(i\text{-}MNT)_2]^{2-}$, has not led to isolated products. Unfortunately, structural comparisons between the $[Au(PPh_3)]^+$ adduct and the analogous planar $[Au_2(i\text{-}MNT)_2]^{2-}$ cannot be made at this time since this latter material has not been isolated.

Acknowledgment. This work has been supported by the National Science Foundation (Grant CHE 8708625), the NSF-REU program, and the Robert A. Welch Foundation. R.M.D. also gratefully acknowledges the receipt of a General Electric Foundation Teaching Incentive Grant, and A.E. acknowledges a Ministerio de Educación y Ciencia fellowship from the Fulbright Commission.

Supplementary Material Available: For 1–4 tables of crystallographic data, atomic coordinates, thermal parameters, and bond distances and angles (38 pages). Ordering information is given on any current masthead page. Tables of F_o and $\sigma(F)$ (80 pages) are available from J.P.F. upon request.

---

(35) Wang, S.; Fackler, J. P., Jr. *J. Chem. Soc., Chem. Commun.* **1988**, 22.

(36) A reviewer has taken issue with the use of the term "relativistic bond" or "relativistic metal–metal interaction". Clearly, the interaction is a result of the relativistic contraction of the metal s orbitals and the subsequent expansion (by shielding) of the filled metal d orbitals, a phenomenon which maximizes at gold for the nonradioactive elements. Since the interaction is a direct result of these relativistic effects, the term relativistic gold bond is just as sensible as "hydrogen bond" for the 3-center 2-electron bond in M–H–M systems.